International Journal of Heat and Mass Transfer 52 (2009) 5285–5292

Contents lists available at ScienceDirect

International Journal of Heat and Mass Transfer

journal homepage: www.elsevier.com/locate/ijhmt

Effect of pulsed magnetic field on superalloy melt

Xiaoping Ma, Yuansheng Yang *, Bin Wang

Institute of Metal Research, Chinese Academy of Sciences, Shenyang 110016, China

ARTICLE INFO

Article history:
Received 24 December 2008
Received in revised form 1 June 2009
Accepted 24 June 2009
Available online 27 August 2009

Keywords:
Pulsed magnetic field
Transient finite element analysis
Magnetic force distribution
Flow field
Joule heat distribution

ABSTRACT

In order to investigate the magnetic force distribution, flow field distribution and Joule heat distribution under the pulsed magnetic field (PMF), transient numerical simulation was carried out. Results show that the magnetic pressure force appears in the inner of the melt, while the magnetic pull force and the magnetic pressure force appear alternately in the exterior of the melt, which is caused by the skin vortex current. The axial direction magnetic force results in the convection of the melt. The radial direction magnetic force produces vibration of the melt. The vibration will diffuse and superpose to produce the pressure wave. Finally, the fluctuation of the melt is caused by the pressure wave. The Joule heat produced by pulsed magnetic field concentrates near the surface of the melt in the pulse applying period.

1. Introduction

The microstructure can be refined by the electromagnetic field applied in the solidification process, which will improve the properties of casting. It is notable that electromagnetic vibration can significantly refine solidified microstructure [1–6]. Recently, pulsed magnetic field (PMF) was applied to microstructure refinement and showed significant refinement effect [7–9]. The PMF is favorable because it is simple in equipment and easy to control. However, the variation of magnetic force and the flow field distribution with the magnetic pulse in the whole period is not clear because the PMF is transient, variable and complex. Because of experimental restriction, it is hard to solve those questions through experiment observation. But numerical simulation provides an effective analysis for experiment and industry production. The numerical analysis can contribute to understanding the mechanism why the PMF can refine microstructure. Kolesnichenko et al. simulated the magnetic force and the flow distribution under PMF produced by sine wave current, and the variation in the pulse applying period was investigated [10]. But the variation in the whole period needs to be further investigated. Besides the magnetic force and the flow distribution, the Joule heat produced by the PMF should also be investigated. In this work, the magnetic force distribution, the flow distribution, and Joule heat distribution in the nickel-based superalloy melt under 2.5 Hz PMF produced by the capacitor are researched in the whole pulse period using commercial Ansys finite element software.

* Corresponding author. Tel.: +86 024 23971728; fax: +86 024 23844528.
E-mail address: ysyang@imr.ac.cn (Y. Yang).

0017-9310/$ - see front matter
doi:10.1016/j.ijheatmasstransfer.2009.06.042

2. Mathematical model

2.1. Physical entity and parameter

The PMF casting setup and FEM model used in the simulation are shown in Fig. 1. The PMF casting setup is consisted by the PMF coil, the mold and the melt. We build the FEM model according the PMF casting setup. The current in the coil is a half sine wave, and the pulse current time is 2.8 ms, which is very short compared with the whole period time when the simulated PMF frequency is 2.5 Hz. Therefore, the change in the pulse current can be simplified as linear, which is shown in Fig. 2. The current peak is 8700 A. The parameters used in the magnetic force distribution simulation are shown in Table 1. In the calculation of the flow field distribution, the melt density is 7800 kg/m^3, and the viscosity is 0.0073 Pa s.

2.2. Governing equations

The governing Maxwell equations of electromagnetic field can be expressed in following equations:

$$\nabla \times E = -\partial B/\partial t \quad (1)$$
$$\nabla \cdot B = 0 \quad (2)$$
$$\nabla \cdot D = \rho_0 \quad (3)$$
$$\nabla \times H = J + \partial D/\partial t \quad (4)$$

The constitutive relations for the related electric fields are described in the following equations:

Nomenclature

B	magnetic flux density vector [Wb m^{-2}]
C_p	specific heat [J kg^{-1} K^{-1}]
D	electric flux density vector [C s^{-2}]
E	electric field intensity vector [V m^{-1}]
f	electromagnetic force [N]
H	magnetic field intensity vector [A m^{-1}]
J	total current density vector [A m^{-2}]
K	thermal conductivity [J kg^{-1} K^{-1}]
p	pressure [Pa]
Q_v	volumetric heat source [J m^{-3} s^{-1}]
t	time [s]
T	temperature [°C]
t_{ij}	stress tensor
u_i	orthogonal velocities ($u_1 = v_x$, $u_2 = v_y$, $u_3 = v_z$) [m s^{-1}]
v	velocity vector [m s^{-1}]
v_x, v_y, v_z	velocity vector components in the x, y and z directions [m s^{-1}]
x, y, z	global Cartesian coordinates

Greek symbols

ε	permittivity [F m^{-1}]
λ	second coefficient of viscosity [kg m^{-1} s^{-1}]
μ	dynamic viscosity [kg m^{-1} s^{-1}]
μ_0	magnetic permeability [H m^{-1}]
ρ_0	electric charge density [C m^{-3}]
σ	conductivity [Ω^{-1} m^{-1}]

Subscripts

I	electric current
MN	minimal value
MX	maximal value
t	time
x, y, z	global Cartesian coordinates

$$J = \sigma(E + v \times B) \tag{5}$$

$$D = \varepsilon E \tag{6}$$

$$B = \mu_0 H \tag{7}$$

The Lorentz force can be acquired according to the following equation:

$$f = \mu_0 J \times H \tag{8}$$

The continuity equation, the momentum equation and the incompressible energy equation are described in Eqs. (9)–(11), respectively.

$$\frac{\partial \rho}{\partial t} + \frac{\partial(\rho v_x)}{\partial x} + \frac{\partial(\rho v_y)}{\partial y} + \frac{\partial(\rho v_z)}{\partial z} = 0 \tag{9}$$

$$\tau_{ij} = -p\delta_{ij} + \mu\left(\frac{\partial u_i}{\partial x_j} + \frac{\partial u_j}{\partial x_i}\right) + \delta_{ij}\lambda\frac{\partial u_i}{\partial x_i} \tag{10}$$

$$\frac{\partial}{\partial t}(\rho C_p T) + \frac{\partial}{\partial x}(\rho V_x C_p T) + \frac{\partial}{\partial y}(\rho V_y C_p T) + \frac{\partial}{\partial z}(\rho V_z C_p T) = \frac{\partial}{\partial x}\left(K\frac{\partial T}{\partial x}\right) + \frac{\partial}{\partial y}\left(K\frac{\partial T}{\partial y}\right) + \frac{\partial}{\partial z}\left(K\frac{\partial T}{\partial z}\right) + Q_v \tag{11}$$

The boundary conditions consistent with the physical entity shown in Fig. 1 are as follows:

Melt top surface $V_y = 0$;
Melt bottom and side surface $V_x = 0$, $V_y = 0$;
Symmetry axis $V_x = 0$.

3. Numerical procedure

Because the PMF is transient and variable, the time dependent simulation is applied. In the simulation, 50 steps are calculated in the periods I, II, IV and V, and the time step is 0.0005 s in the period III. First the vector potential method is applied to calculate the electromagnetic field to get the force distribution and then the result for the magnetic force is coupled with the flow field transient simulation. The plane 53 element is used in the electromagnetic simulation, and 2D flotran 141 element is used in the flow field simulation. The flow field distribution is calculated using the tri-diagonal matrix algorithm [11] (TDMA) iterative solver with laminar model.

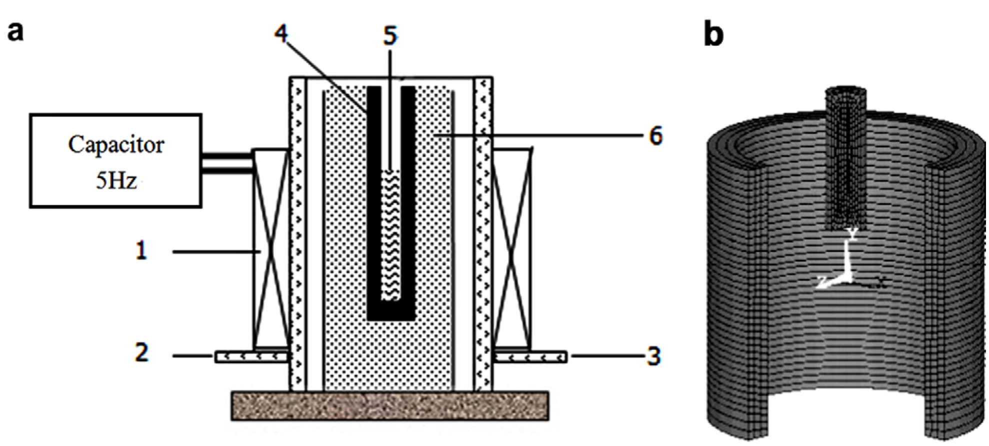

Fig. 1. Sketch of PMF casting setup (a) and FEM model used in the simulation (b). 1. Generator of the pulsed magnetic field, 2. Cooling water inlet, 3. Cooling water outlet, 4. Mold, 5. Melt, 6. Refractory.